International Conference on Space Optics—ICSO 2018

Chania, Greece

9–12 October 2018

Edited by Zoran Sodnik, Nikos Karafolas, and Bruno Cugny

SCALE: validations and prospects for a novel type of sounding lidar using short frequency combs

Philippe Hébert

François Lemaître

International Conference on Space Optics — ICSO 2018, edited by Zoran Sodnik, Nikos Karafolas, Bruno Cugny, Proc. of SPIE Vol. 11180, 111801T · © 2018 ESA and CNES · CCC code: 0277-786X/18/$18 · doi: 10.1117/12.2535984

SCALE: validations and prospects for a novel type of sounding lidar using short frequency combs

Philippe J. Hébert[*a], François Lemaître[b]
[a]CNES, 18 av. E. Belin, 31401 Toulouse, France; [b]ONERA, 2 av. E. Belin, 31400 Toulouse, France

ABSTRACT

As compared to near InfraRed passive instruments, lidars reduce the biases on the measurement of concentrations in the presence of diffusion by aerosols, but until recent days they were limited to one active wavelength at a time.

CNES and ONERA conceived a novel type of lidar based on short frequency combs that provides the spectrum of a complete absorption line of the target molecule. The technique of Dual Comb Spectroscopy is adapted to short (up to 13 teeth) combs, as a compromise between spectral richness and Signal to Noise Ratio. The advantages of DCS remain: reduction of the impact of scene evolutions and spectral mis-calibration. The latter will make the high power laser emitters easier. Above all, the acquisition of a complete absorption line opens the path to the retrieval of two or more independent elements in the vertical profile of molecule concentration.

We describe the technique of comb generation, the layout of the emitter section and the detection principles. Then we introduce the Short Comb Atmospheric Lidar Experiment (SCALE) project led by CNES in the frame of a new advance "phase 0" study. We expose the preliminary performances of this space lidar that could fit on a microsatellite platform in the case of CO_2 sounding at 1.57 or 2 µm.

Results of CNES-ONERA four-year R&T activities are also presented that validate in the laboratory and in open space the short comb lidar.

Finally first results of retrieval simulations are exposed.

Keywords: lidar, spectroscopy, atmospheric sounding, frequency combs

1. INTRODUCTION

Until recently DIfferential Absorption Lidar (DIAL) sounding space lidars were limited to one or two active wavelengths [1]. This poor frequency information restraints the concentration retrieval to one vertical element, namely the integrated column amount. And the accurate retrieval of the molecule concentration puts hard constraints on the knowledge of key parameters as actual emitted wavelength [9] or other geophysical parameters [10].

On the other hand passive space instruments as spectrometers or interferometers provide complete spectra of the atmosphere in the UV [2], visible [3] or infrared wavelengths [5] [6]. They allow the retrieval of temperature or humidity profiles [4], several molecule concentration and green house gazes as CO_2. But thermal infrared wavelengths do not allow accurate measurements of the concentration of CO_2 ($[CO_2]$) down to the troposphere, and visible or near infrared wavelengths are limited to day-time measurements. They are also impinged by the aerosol and cloud diffusion of the optical flux that introduce inaccuracy in the distance crossed through by the flux, thus in the concentration calculated from the attenuation measurement. This results in geographical biases in lidar measurements that call for correction.

Proposed by CNES and ONERA, the concept of frequency comb lidar aims at joining the advantages of lidar and spectrometer instruments together. It is basically a lidar, but it features a set of inter-calibrated wavelengths. Doing so allows to withdrawn the diffusion bias, together with providing a real spectrum of the transmitted flux. The expected end

advantages are a non-biased concentration of the targeted molecule in the atmosphere and possibly some information on its vertical distribution.

2. ABSORPTION LINE PROFILING

The new short frequency comb lidar aims at providing the spectrum profile of a single absorption line of a target molecule in the atmosphere. The way it scans such a line is a clue in the field of lidar instruments.

2.1 Sequential scanning

Some frequency agility is permitted by an Optical Parametric Oscillator (OPO) used in the emitter. This allows sounding of different species so as to eliminate the unknown content of H_2O when looking for CO_2 for instance [14]. But for each species the active wavelength is single.

One way to remedy this limitation is to multiply the emitted wavelengths along one absorption line [7]. A scan takes few ms to perform. The improvement of the spectral content allows a better retrieval of CO_2, with some information in the vertical profile [8] [11]. However in a space mission the reflectivity of the ground would not be the same for all wavelengths and the pointing of the telescope should be stabilized. Aerosol conditions may change too as sketched by Figure 1:

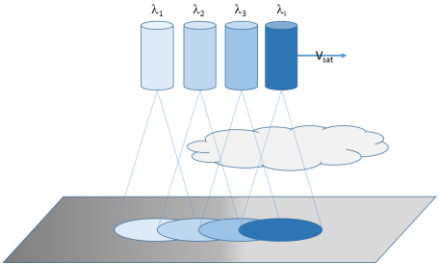

Figure 1. Sequential wavelength scanning for a space borne lidar

Finally the wavelength of the master laser must be accurately stabilized or monitored during the scan, as for DIAL lidars.

2.2 Short frequency combs

Short frequency comb lidars are based on the principle of emitting a set of wavelengths similar to [11] but at the same time, and with an even and accurately known frequency step.

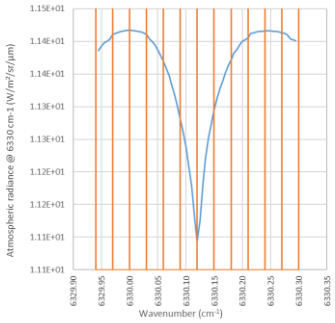

Figure 2. Short frequency (or wavelength) comb used to sample one spectral line c.a. 6330 cm^{-1}

Even if the center frequency may shift, the absorption line is sampled at evenly spaced frequencies. Therefor the shape of the line is determined anyway. This relaxes the mastering of the central wavelength.

Finally all these wavelengths are detected by the same detector, as in a Michelson interferometer, with a reduced frequency bandwidth.

As a matter of fact the number of frequencies in a comb is a compromise between spectral richness, thus the quality of the concentration retrieval, and the energy of each one, hence the Signal to Noise Ratio in the spectrum, keeping in mind the limit of the available total energy onboard.

3. DCS TECHNIQUE

3.1 Dual (Short) Comb Spectroscopy

Dual Comb Spectroscopy (DCS) is now a well-known technique for fast, high resolution, large spectral domain spectroscopy [12] [13]. Since its debuts in the laboratory it was experienced to use it in open space (lidar mode) on the distance of few km [15]. DCS involves usually several hundreds of thousands teeth, spanning several nm spectral domains, and uses phase locked femtosecond (fs) lasers.

It involves two frequency combs, with a slightly different step. Thus the frequencies of comb #1 are $\upsilon_{op}+i.fr_1$, and the frequencies of comb #2 are $\upsilon_{op}+i.fr_2$. υ_{op} being the optical carrier frequency (in the order of 200 THz).

Complete frequency combs are a thrilling perspective for lidars, but their fitting to a space mission is beyond the state of the art of today's short (fs) pulse optical amplifiers. In the case of short combs the feature is more modest, and the technique of comb generation is different, but the principles are the same for the spectroscopic point of view. Here $1 \leq i \leq 13$. $fr_1 \sim fr_2$ are chosen to cover the molecule absorption line. Typically $fr_1 \sim fr_2 \sim 1$ GHz, and $\Delta f_r = fr_1 - fr_2 \sim 1$ MHz.

Both combs are amplified and sent through the atmosphere, are reflected back by a hard target, cross the atmosphere again, and are superimposed onto a detector. This generates a multi-heterodyne beat-note signal, at RF (Radio Frequency) frequencies $i.\Delta f_r$. Higher frequencies $i.(fr_1+fr_2)$ and $i.fr_1-j.fr_2$ or $i.fr_1+j.fr_2$ are filtered out by a Low Pass Filter.

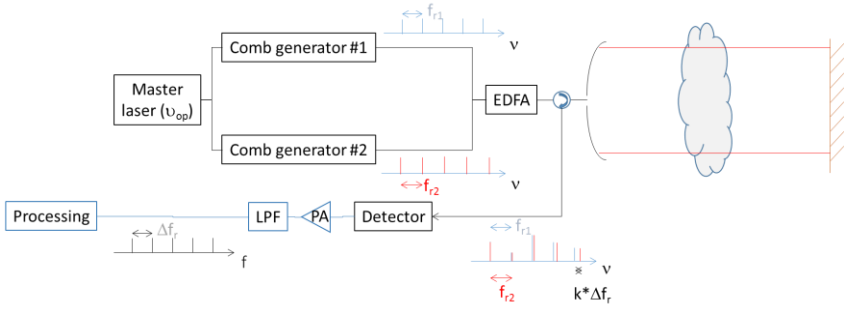

Figure 3. General layout of a short comb lidar. EDFA: Erbium Doped Fiber Amplifier - PA: PreAmplifier – LPF: Low Pass Filter. Black: Polarization Maintaining (PM) fiber optics links – Red: open space optical path – Blue: electronic signal – υ: optical frequency – f: RF electronic frequency

3.2 Interferogram and spectrum

As both combs are generated from the same master monofrequency laser, the phase between them is stable and the beat-note builds up constructively. The optical total amplitude can be written as:

$$A_{tot}(t) = \sum_{k=0}^{N} A_1(\upsilon_{op} + k.fr_1).e^{j.2.\pi.k.fr_1.t} + \sum_{k=0}^{N} A_2(\upsilon_{op} + k.fr_2).e^{j.2.\pi.k.fr_2.t} \quad (1)$$

since we can neglect higher frequency terms thanks to the LPF. N is the number of frequency teeth.

$A_1(\upsilon_{op}+k.fr_1)$ and $A_2(\upsilon_{op}+k.fr_2)$ are the amplitudes of the optical flux at optical frequencies $\upsilon_{op}+k.fr_1$ and $\upsilon_{op}+k.f_{r2}$, after crossing the atmosphere twice. "A" is closely related to the spectral transmission and is the parameter we are looking for. As $fr_1 \sim fr_2$, we can approximate and write: $A_1(\upsilon_{op}+k.fr_1) = A_2(\upsilon_{op}+k.fr_2) = A_k$ in equation (1).

The intensity $I_{tot}(t) = A_{tot}(t).A_{tot}(t)^*$ can be derived from equation (1) as:

$$I_{tot}(t) = 2.\sum_{k=0}^{N} A_k.[1 + \cos(2.\pi.k.\Delta f_r.t)] \quad (2)$$

$I_{tot}(t)$ constitutes an interferogram signal similar to the one of a Michelson interferometer like [4].

The electrical signal is proportional to $I_{tot}(t)$ and equation (2) shows that it is the inverse Fourier Transform of $A_k = A_1(\upsilon_{op}+k.fr_1) = A_2(\upsilon_{op}+k.fr_2)$ series. So the processing consists in digitalizing the signal and calculating its Fourier Transform. $A(f) = TF[I_{tot}(t)]$ is the spectrum in the RF domain. It must be translated to the optical domain by $A(\upsilon_{op} + k.f_r) = A\left(f.\frac{f_r}{\Delta f_r}\right)$ as the amplitude of A_k appears at the RF frequency component $k.\Delta f_r$ in equation (2).

One interesting feature of DSC is inferred from equation (2). As $I_{tot}(t)$ is the superposition of harmonic phase locked components, it is periodical with a repetition rate of $\frac{1}{\Delta f_r}$. This is illustrated by Figure **4** and can be demonstrated by:

$$I_{tot}\left(t+\frac{1}{\Delta f_r}\right) = 2.\sum_{k=0}^{N} A_k.\left[1+\cos\left(2.\pi.k.\Delta f_r.\left(t+\frac{1}{\Delta f_r}\right)\right)\right] = 2.\sum_{k=0}^{N} A_k.[1+\cos(2.\pi.k.\Delta f_r.t)] = I_{tot}(t)$$

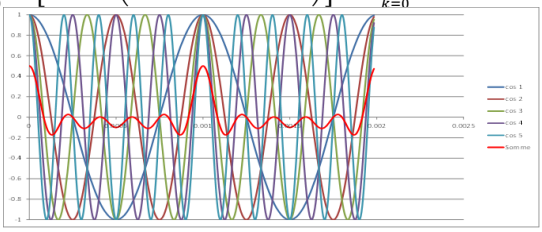

Figure 4. Superposition of harmonic phase locked components. Red: resulting total signal

This repetition makes it easy to average several acquisitions with no moving part in the instrument as long as the target is stable.

3.3 Spectral resolution and sampling

Each interferogram is monitored in the $\left[-\frac{1}{2.\Delta f_r};+\frac{1}{2.\Delta f_r}\right]$ temporal interval. As with passive interferometer the spectral resolution is the Full Width at Half Maximum (FWHM) of the Fourier transform of the box-car truncation function of the interferogram. As a consequence, the FWHM of the instrument (sinc) function is $1.21.\Delta f_r$ in the RF domain, and $1.21.f_{r1} \sim 1.21.f_{r2}$ in the optical domain. But it must be outlined that the useful spectrum is empty between the very narrow comb teeth. Even if the final spectrum is the physical spectrum convoluted by the instrument function, no lateral component but of the solar background is aliased in the considered channel as zeros of the instrument function coincide with the adjacent teeth when $T_{obs} = \frac{1}{\Delta f_r}$, as shown by Figure **5**:

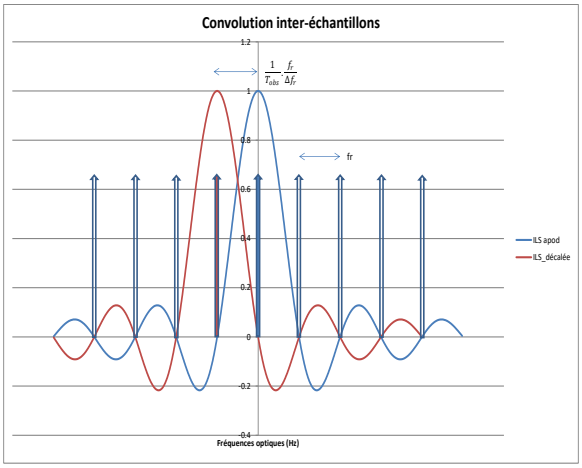

Figure 5. Inter-sample convolution. Comb teeth are symbolized by arrows. Red and blue: instrument functions of two adjacent samples

The samples of the spectrum can be considered as polluted only by the solar spectrum adjacent components, but these are of low level and independent one another. This is a peculiar property of DCS.

Each tooth of the comb is as narrow as few kHz, depending on the spectral purity of RF wave injected in the optical modulators. In the optical domain they are spaced by $f_{r1} \sim f_{r2}$, of the order of 1 GHz here, i.e. 7.5 pm at 1.5 µm, i.e. 0.033 cm^{-1} at 6600 cm^{-1}.

3.4 Generation of short frequency combs

Short frequency combs can be generated from a cw mono-wavelength laser using an Electro-Optic Modulator (EOM) for phase modulating of the master laser. When passing through an EOM driven by a voltage V = b.sin(ωt+φ), the laser phase i.ω_0.t becomes i.(ω_0.t + b.sin(ωt+φ)) as can be seen in Figure **6**:

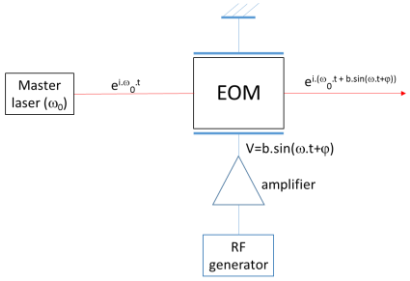

Figure 6. Phase modulation of a Master Laser with an EOM

The building of short frequency combs from such a phase modulation is presented in § 5.1.

There are two positive technical consequences to the use of frequency combs. First the frequency step is highly stable, even, and mastered, being generated by RF ultra-stable oscillators. Secondly it spreads the total energy within several frequencies, lowering the level of each of them with respect to the Brillouin's scattering threshold in the fiber amplifiers.

3.5 Emitter architecture

The instrument relies on two branches similar to Figure **6**, branch #1 having F = fr_1 and branch #2 having F' = fr_2. However one of the combs generated has to be shifted so as to avoid ambiguity of beat-notes i.Δf_r. and –i.Δf_r, around the central original frequency, as can be seen in Figure **7**:

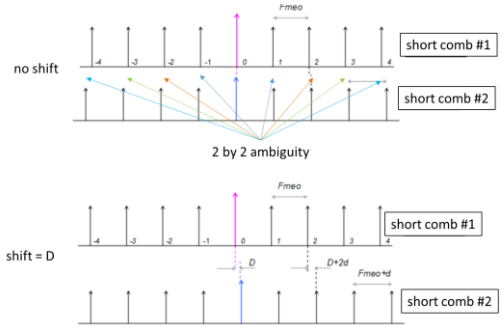

Figure 7. Global frequency shift of one comb

At first order, D must be equal to $D = \frac{(N+1)}{2}.\Delta f_r$ so that no tooth of the two combs superimpose and give birth to the same beat note tone.
Practically speaking, a global shift is provided by an Acousto-Optic Modulator (AOM). As AOMs don't work around D.C. but around 110 MHz, comb #1 is shifted by 110 MHz – D/2 and comb #2 is shifted by 110 MHz + D/2.

The complete diagram of the emitter gathers the above considerations in Figure **8**:

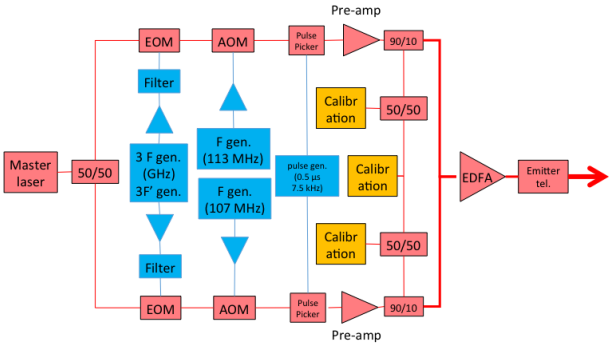

Figure 8. Complete emitter diagram for a short comb lidar

A pulse picker is introduced in each branch to allow a pulse emission mode according to allow time tagging of the echoed pulse.

The calibration channels measure the energy spectra actually emitted to correct the echo signal from emitter discrepancies.

3.6 Detection and processing

Detection of the interferogram is straightforward as a low bandwidth detector (few MHz) is sufficient. It must be followed by a LPF of which cut-off frequency is at maximum half of f_r to avoid aliasing in the spectrum. In our case $f_r/2$ is much higher than our maximum useful frequency $N.\Delta f_r$. This is why the LPF cut-off frequency is set just above $N.\Delta f_r$ in order to limit the noise bandwidth.

The sampling of the interferogram is made at twice $N.\Delta f_r$, at least, with a resolution sufficient to generate negligible noise. Averaging of several interferograms can be made, then a Fourier Transform is performed to finally obtain up to 13 samples in the absorption line of the target molecule [17].

4. INTRODUCING SCALE: SHORT COMB ATMOSPHERIC LIDAR EXPERIMENT

CNES propose a new member in the family of space lidars based on the above principles: the Short Comb Atmospheric Lidar Experiment (SCALE). In this chapter we address the limits of a mission adapted to a micro-satellite like Myriade Evolution bus [18]. Its interface section with the payload is in the order of 100 cm × 100 cm. It allows a telescope of 0.7 m diameter and a power of 150 W to the payload. The following paragraphs present a first order radiometric exercise for such a mission.

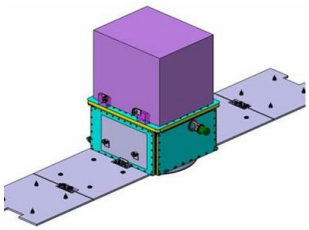

Figure 9. Myriade Evolution Platform. The payload volume is in purple.

4.1 SCALE objectives

SCALE is viewed as a demonstration mission for CO_2 sounding with a short comb lidar, in the 1.57 µm or 2 µm region. The measurements are averaged along a cell on the ground of 50 km long. Its width should be few hundred meters. The number of spectral samples will be between 3 and 13, the optimum remains to be determined. The spectra should allow retrieving more independent elements in the vertical profile (Degree Of Freedom For Signal "DOFFS") than a DIAL lidar.

4.2 SCALE key parameters

The spectral parameters of the combs were given in § 3.

The radiometric performances are driven by the following factors. The most important one is the energy of each laser pulse. Assuming that one third of the 150 W delivered by the platform is dedicated to one comb amplifier, assuming an electro-optic efficiency of 35% for the pump laser diode, and taking into account the opto-optical efficiency of 21% [19], we consider an optical power of 3.7 W for each comb. Given the repetition rate of F_{rep}=7.2 kHz (consistent with the non-ambiguous range of 40 km required for atmospheric sounding from space) this power yields to a E_0=0.5 mJ energy per pulse and per comb. Of course this energy is spread over the N teeth of a comb. The pulse duration is t_{pulse}=0.5 µs.

The altitude is lowered to R_0=400 km. The receiver telescope diameter is 0.7 m. We consider the ground reflectivity to be Ref=0.1 sr^{-1}. The total atmospheric optical depth is taken to 0.5 which leads to an atmospheric transmission of T_{atm}^2=0.6, typical of the edge of a CO_2 transmission line in the near infrared. The optical transmission of the receiver is T_{inst}=0.7 and the one of the emitter T_{emit}=0.9. The background parasitic flux is determined by the Solar Zenithal Angle (SZA) of 60°.

The detector is granted a top of the art performance with a Noise Equivalent Power (NEP) of 5 fW/√Hz including the preamplifier. Its efficiency is η=0.8.

4.3 SNR in the interferogram and in the spectrum

Assuming that the noise in the interferogram is white and non-correlated, the Signal to Noise Ratio (SNR) in one channel (of width df) in the RF spectrum (which is the same as for the optical spectrum) is given from the SNR at the central sample of the interferogram by:

$$\frac{Signal}{Noise}(spectrum)(f) = \frac{S_{TF}(f).df.\sqrt{N}}{2.\int_0^{f_{Max}} S_{TF}(f).df}.\frac{Signal}{Noise}(Interferogram)(0) \quad (4)$$

f_{Max} is the maximum frequency in the interferogram and S_{TF}(f) is the Fourier Transform of the interferogram.
Equation (4) can be simplified if we define S_{TF}^{av} as the average value of S_{TF}(f):

$$\frac{Signal}{Noise}(spectrum)(f) = \frac{S_{TF}(f)}{2.S_{TF}^{av}}.\frac{1}{\sqrt{N}}.\frac{Signal}{Noise}(Interferogram)(0) \quad (5)$$

4.4 Signal

The central sample of the interferogram receives all the frequencies in phase, so only one frequency can be considered with energy E_0 when emitted. This sample is acquired during a time defined by the maximum RF frequency in the interferogram according to the Nyquist frequency as $t_{int} = \frac{1}{2.N.\Delta f_r}$.

This allows the calculation of the number of detected photon-electrons, from one comb, in the central sample of the interferogram according to the "lidar formula":

$$N(R_0) = \frac{\eta.E_0.T_{emit}.A.T_{inst}}{h.\nu L}.\frac{T_{atm}^2}{{R_0}^2}.Ref.\frac{t_{int}}{t_{pulse}} \quad (6)$$

h.υL is the energy of the photon at frequency υL.
2.N(R_0) determines the "signal" of the SNR expression since two combs fall onto the detector.

4.5 Solar background

The number of photon-electrons from the Sun through the atmosphere is

$$N_{BG}(R_0) = \frac{\eta.\pi.\theta_c^2.A.T_{instr}.L_{sun}(1.5\mu m).\Omega_{sun}.\cos(SZA).T_{atm}^2.Ref.\Delta\lambda}{h.\nu L}.t_{int} \quad (7)$$

with: L_{sun}=radiance of the Sun, Ω_{sun}=Sun solid angle, Δλ=width of the Narrow Optical Filter (NOF).
A NOF is inserted in front of the detector to limit the optical bandwidth of the sun flux. Its transmission is included in T_{inst}. We consider Δλ=2 nm.
The larger the field of view θ_c, the larger the background flux, hence the noise. In reality the field of view of the receiver is somewhat bigger than the divergence of the laser to get some margins for misalignments. We consider a margin of 50 %: $\theta_c = \theta_L \times 1.5$. A compromise was found against speckle noise around θ_L = 40 µrd.

4.6 Noises

Addressing the limits of the SCALE concept, we do not take into account the electronics noises in this preliminary budget.

As for natural noises, we take into account the following variances:

- Quantum noise: $var(N(R_0))_Q = 2.N(R_0)$. Factor 2 is for two combs.
- Speckle noise: $var(N(R_0))_S = 2.\frac{N(R_0)^2}{M}$ with M = number of speckle patterns. In our case M ~ 200. The larger the divergence of the laser θ_L, the larger the number of speckle patterns.
- Solar background: $var(N_{BG}(R_0))_{BG} = N_{BG}(R_0)$
- Detection noise: $var(N)_D = \frac{t_{int}}{2}.\left(\frac{\eta.NEP}{h\nu L}\right)^2$
- Total noise: $var(N)_{total} = var(N(R_0))_Q + var(N(R_0))_S + var(N_{BG}(R_0))_{BG} + var(N)_D$ (8)
- Interferogram SNR: prior to use equation (5) we calculate $\frac{\text{Signal}}{\text{Noise}}(\text{Interferogram})(0) = \frac{2.N(R_0)}{\sqrt{var(N)_{total}}}$. Factor 2 stands for the similar one of equation (2).

4.7 Turbulences

Turbulences affect both combs the same way. Therefore their superimposition in the pupil of the instrument should keep a high efficiency close to 1.

4.8 Polarization

As long as the optical fibers and elements of the instrument are of the Polarization Maintaining (PM) type, theory and experience show that polarization is not an issue for the stability of the signal. And the effect of the atmosphere on the optical beam polarization will be the same for the two combs, if any, so no perturbation in the heterodyne beat notes is to be feared.

4.9 Averaging

In this first evaluation we consider that the target is constant over D_{av}=50 km, so averaging of $N_{av} = \frac{D_{av}}{V_{sat}}.F_{rep}$ measurements (with V_{sat}=7.5 km/s velocity of the satellite) will increase the SNR by a factor $\sqrt{N_{av}}$.

4.10 Preliminary radiometric budget

The simple model above gives the preliminary estimate of the SNR, in each channel of the spectrum. Figure **10** summarizes the results of SNR calculation with the above assumptions, as a function of optical power of one comb, for several numbers of teeth.

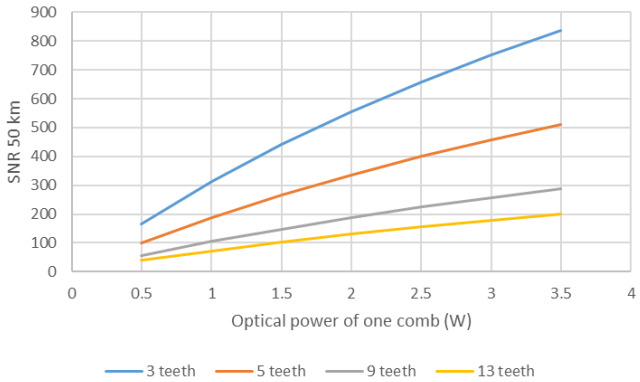

Figure 10. SNR in the SCALE spectrum, for an average along 50 km, as a function of optical power of one comb, for several numbers of teeth. See text for the parameters of the radiometric budget.

As expected the SNR increases with the optical power and decreases with the number of teeth.

Interestingly enough the influence of the solar background is weak with a SZA of 60°: day-time SNR is 6% lower than night-time SNR.

4.11Discussion and ways forward

This work estimates the first order SNR one can reasonably hope for a short comb lidar fitted to a microsatellite bus. If we assume that the optimum number of teeth would settle at nine and the optical power, all loss taken into account, at 3 W per comb, the SNR would be 250 in day-time, after a 50 km averaging.

With these parameters the distribution of variances of equation (8) is shown by Figure **11**:

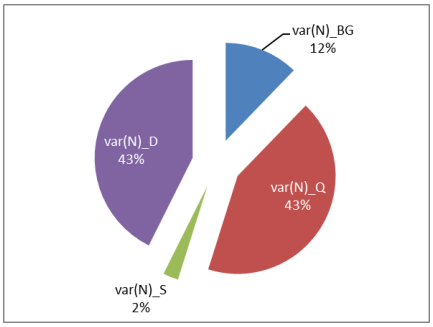

Figure 11. Distribution of noises in the interferogram with 3 W optical power and 9 teeth per comb.

The speckle noise is negligible and the background noise is low, but Figure **11** shows that the instrument is not yet photon-limited. Some progress should be envisaged there.

With key parameters consistent and in line with a microsatellite bus size, SCALE appears to be an instrument with performance perspectives interesting enough for an exploratory mission in the future, to demonstrate a new type of atmospheric active sounding.

5. EXPERIMENTAL VALIDATIONS

During four years ONERA led CNES's R&T activities to experimentally validate the concept of short frequency comb spectroscopy, first in the laboratory with a HCN cell, then in an open space lidar mode.

5.1 9 and 13 teeth combs

We conducted calculations to optimize the generation of 9 and 13-tooth combs using an EOM driven by a wave consisting of a fundamental frequency and its harmonics. Decomposed into Bessel functions the spectrum of such a phase is given by:

$$e^{i.\omega_0.t+i.b.\sin(\omega.t+\varphi)} = e^{i.\omega_0.t}.\left[J_0(b) + \sum_{k=1}^{\infty} J_k(b).e^{i.k.(\omega.t+\varphi)} + \sum_{k=1}^{\infty}(-1)^k.J_k(b).e^{-i.k.(\omega.t+\varphi)}\right] \quad (9)$$

where $J_k(b)$ are the Bessel functions of the first kind.

Equation (9) gives the result for a simple harmonic modulation that produces a spectrum of ω-pitch lines. In this case, only parameter b (the modulation index) is available to act on the distribution of the lines in the optical spectrum. If we add a second harmonic in the modulating signal, we have a total of 3 parameters (2 amplitudes and a relative phase), and so on for 3 harmonic components.

$$e^{i.\omega_0.t+i.b1.\sin(\omega.t+\varphi 1)+i.b2.\sin(2.\omega.t+\varphi 2)+i.b3.\sin(3.\omega.t+\varphi 3)+\cdots\ldots} \quad (10)$$

In this case, the aim is to optimize the 5 parameters b1, b2, b3, $\varphi 2$, $\varphi 3$ in equation (10), with the help of a in-house optimization software, in order to optimize an overall criterion taking into account i) the dispersion of the levels on the useful lines, ii) the relative power in the useful lines compared to the other lines. In the case of the 9-tooth comb (Figure **12**) a very good result is achieved with only the fundamental frequency and its harmonic 3. In the case of the 13-tooth comb, it is necessary to use in addition the harmonic 2 [16] to obtain a maximum deviation of 0.45 dB between the useful lines (Figure **13**). It can be noted that other optimization criteria could be applied, for example to have the same signal to

noise ratio for each tooth of the comb when analyzing an absorption line. In this case it would be necessary to emit more energy on the central lines.

The experimental results obtained with a high-resolution optical spectrum analyzer correspond substantially to the theoretical results as shown in Figure **14** and Figure **15**. The amplitude and phase settings must be accurate and compensate for the transmission characteristics of the power amplifier. This is facilitated by the use of an AWG sampled at 8 GHz, which performs a digital synthesis of the modulating signal. However, high frequency AWG generators has the drawback of producing unwanted lines and the EOM frequency choices must be adjusted so that these stray lines do not interfere with the measurements.

It should be noted that depending on the temperature of the components (RF power amplifiers deliver about 1 watt) the settings change and so the level of the lines, by about 1 dB, if no temperature regulation is used.

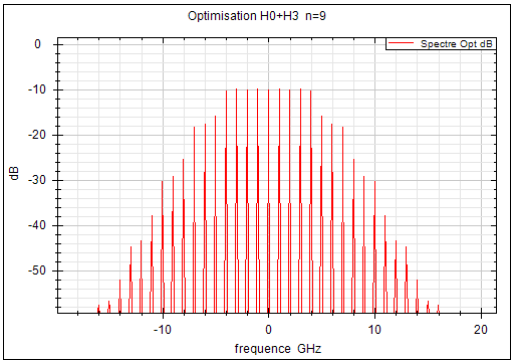

Figure 12. Theoretical optimized 9-teeth mini-comb using a single EOM driven by a fundamental frequency and its third harmonic

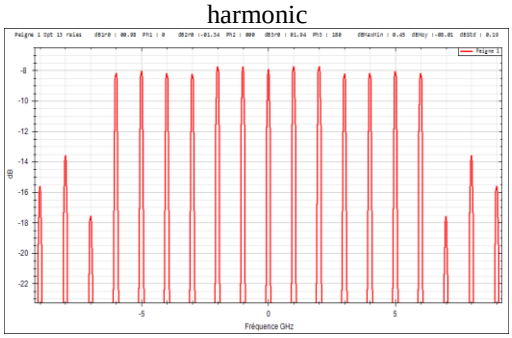

Figure 13. Theoretical optimized 13-teeth mini-comb using a single EOM driven by a fundamental frequency, its second and its third harmonic

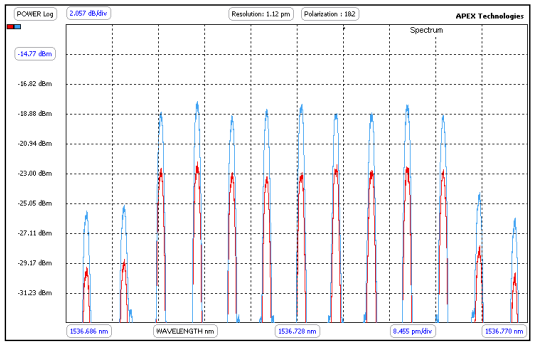

Figure 14. Optical spectrum obtained for the optimized mini comb with 9 teeth. The blue and red tracks correspond to the 2 optical polarizations.

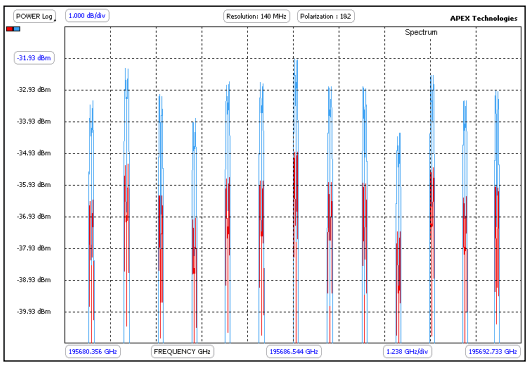

Figure 15. Optical spectrum obtained for the optimized mini comb with 13 teeth. The blue and red tracks correspond to the 2 optical polarizations

5.2 Experimental setup

The experimental set-up in the laboratory is shown in Figure **16** and Figure **17**. The two combs generated are added in a coupler, amplified in an EDFA and then sent in two reception channels: on one side the "measurement" channel which contains the HCN cell and a 10 km non PM fiber which simulates propagation, and on the other side the "reference" channel. The latter keeps in memory the levels actually emitted on each line, which may vary according to time, temperature and the characteristics of the EDFA. However, the transfer functions of the "measurement" and "reference" channels are not exactly identical since they use different components (photo detectors, RF amplifiers, filters). This has been calibrated.

The beats of the homologous lines of both combs show an RF comb centered at the frequency AOM2-AOM1 (here 11.4 MHz) and with an EOM2-EOM1 step (here 0.1 MHz), as shown in Figure **18**. We can notice that these lines are extremely stable because the optical waves that generate them have very close frequencies, travel identical paths at the same time, and have identical polarizations, even if part of the path uses non-PM fibers. Experimentally, stability identical to that of the RF and microwave signals used for the AOM and EOM modulators is observed. This property opens up the possibility of spectral analysis over very long observation times, thus improving the signal-to-noise ratio.

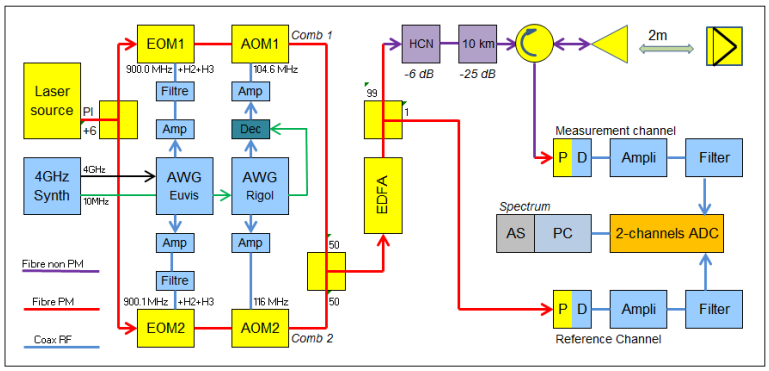

Figure 16. Laboratory set-up: general block diagram.

Figure 17. Laboratory set-up

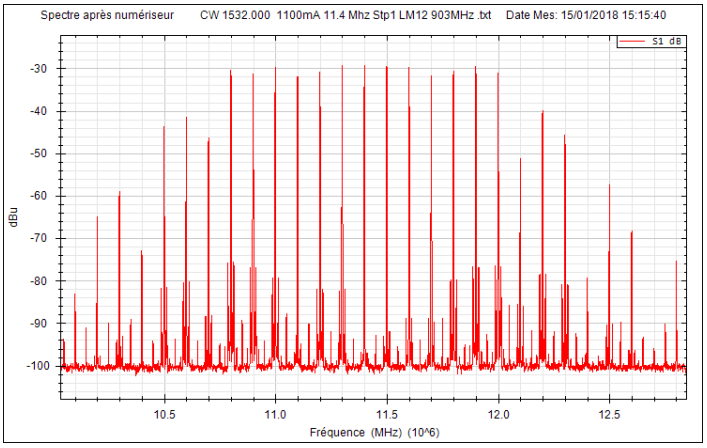

Figure 18. Spectrum at the output of the "reference" channel

5.3 HCN spectra

The general appearance of the spectral transmission of the $H_{13}C_{14}N$ cell (15 cm long, 25 Torr) is shown in Figure **19**. These data are derived from measurements made by the NIST [20].
It should be noted that for our experiment, the two optical waves that beat (at practically the same frequency) are attenuated in the cell, which means that the sensitivity is doubled.
The measurement procedure is as follows: after tuning the source laser to the line to be analyzed, the spectra of the "measurement" and "reference" channels are recorded and the levels extracted from the 13 lines. The difference is then made to compensate for changes in the levels of emitted optical lines.
To facilitate comparison with the NIST results, the measurement points are adjusted with a global level offset that compensates for measurement channel losses and gain differences, as well as a global frequency offset to compensate for source laser drift (typically 100 to 200 MHz).

The results obtained for three lines at 1535.540 nm, 1555.436 nm and 1563.498 nm are shown in Figure **20**, Figure **21** and Figure **22**. For this last measurement, the pitch of the optical combs was reduced from 903 MHz to 303 MHz in order to better sample this absorption line.
We can see on these figures that the obtained results are quite good since we have deviations lower than 0.1 dB. A thorough analysis of these residual or bias errors shows that they can be explained by the parasitic lines generated by the microwave AWG mentioned above.

These results validate the concept of spectroscopy with two short frequency combs for the first time.

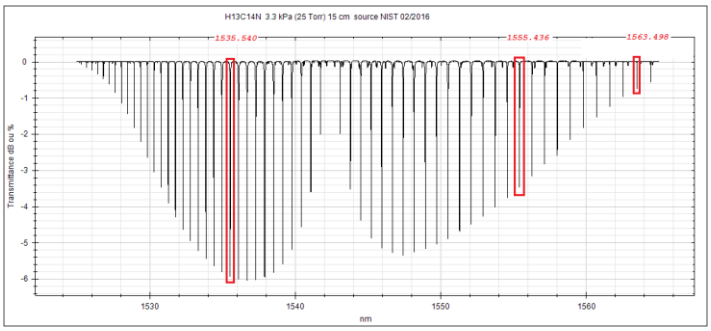

Figure 19. NIST measurements for a $H_{13}C_{14}N$ 15cm long, 25 Torr pressure cell. Red boxes indicate the actually measured absorption lines

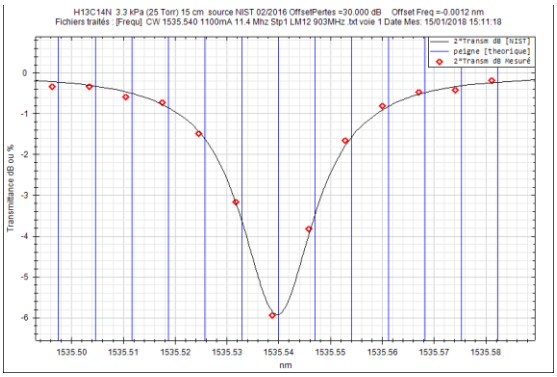

Figure 20. Comparison of our measurements (red dots) and NIST (black continuous line) results for the 1534.540 nm line

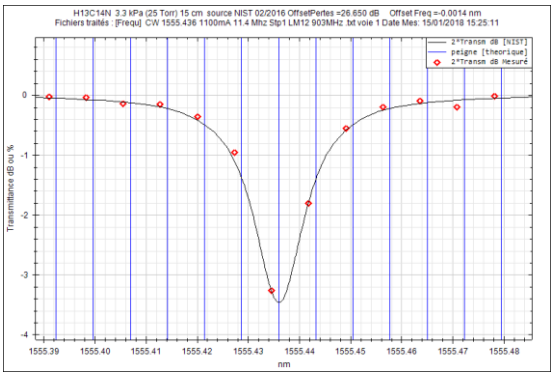

Figure 21. Comparison of our measurements (red dots) and NIST (black continuous line) results for the 1555.436 nm line

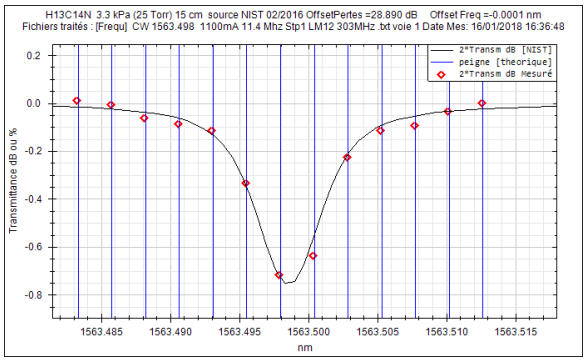

Figure 22. Comparison of our measurements (red dots) and NIST (black continuous line) results for the 1563.498 nm line

5.4 Future works: open space measurements

After these experiments on an HCN fiber absorption cell, it is scheduled to test in open space a lidar based on dual short frequency combs. The functional diagram of the instrument is the one of Figure **16**, but the distance to the retroreflector will be 1 km, horizontal. Moreover we will sound water vapor at 1528.75 nm as there is no CO_2 absorption line strong enough in the C band of our tunable master laser. We expect a transmission of around 45 % as per Figure **24**:

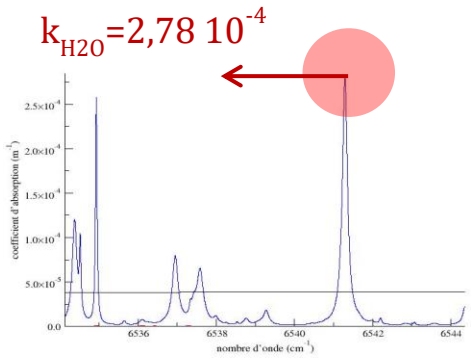

Figure 23. Absorption coefficient of water vapor at the edge of the laser C band

The comparison of the measured spectra to those simulated from in-situ measurements will validate the accuracy of the short comb lidar.

These experiments will shortly take place in the ONERA's facilities of Le Fauga, France.

6. RETRIEVAL

A first study of the processing of CO_2 short comb spectra was led to address the capabilities of SCALE. The simulator used includes different modules of initialization, direct transfer calculation, instrument simulation, inversion module, according to the block-diagram of Figure 24:

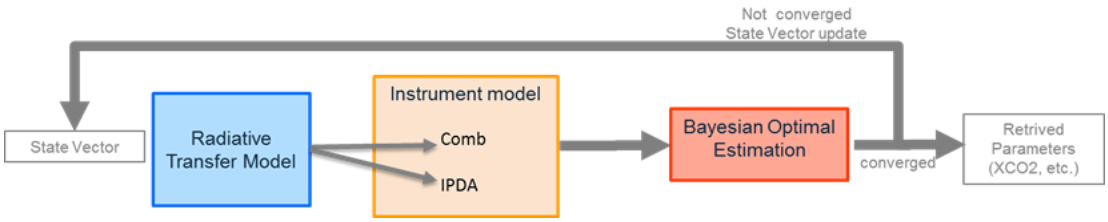

Figure 24. Instrument and processing model

The principle of those simulations is to choose an "actual" atmospheric state vector (mainly, a CO_2 concentration profile), and to start the retrieval simulation with a "prior" state vector. The "prior" state vector is the "actual" one affected by an error σ_{prior}. The final retrieved state vector should have an error σ, with respect to the actual one, so that $\sigma/\sigma_{prior} < 1$. This error is calculated for the whole column and for each of [0 – 3 km], [6 – 9 km]… layer, the lower one being of most importance for the SCALE mission.

The instrument model inputs are the parameters of § 4.2. The number of teeth, the central wavelength, the spectral step was varied to determine an optimized configuration. This research was led around 1.572 µm and around 2.064 µm, as this band contains CO_2 lines as well. In this first study geophysical parameters other than CO_2 content and center wavelength were assumed to be perfectly known.

6.1 Accuracy and DOFFS

The accuracy on the CO_2 retrieved concentration and the DOFFS are calculated for several numbers of teeth in the combs, and for several optical powers per comb: nominal (3.7 W), 2×nominal (5.4 W) etc… This will give perspectives for improving the retrieval. The first results are summarized in Figure **25**:

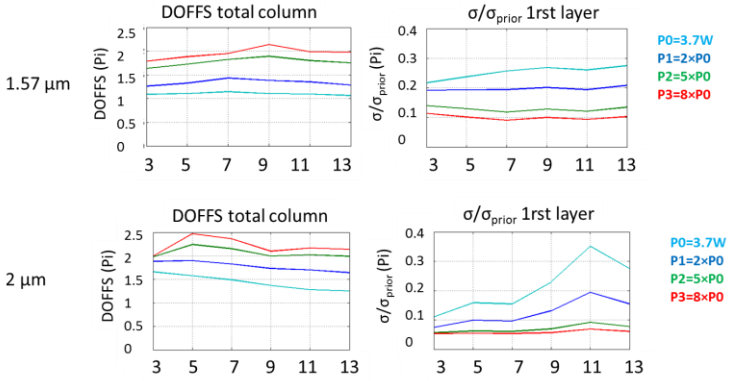

Figure 25. DOFFS in the total column and accuracy for 3 to 13 teeth in the combs (x axis), different optical powers, at 1.57 µm and 2 µm.

It can be seen that performances are slightly better at 2 µm than 1.57 µm. The loss of SNR with higher number of teeth seems balanced by the spectral information content at 1.57 µm. This is no more the case for the accuracy at 2 µm when N > 9. Performances are somewhat better with 3 teeth but some phenomena are neglected like [H_2O] uncertainty. However other calculations show that there is less correlation between atmosphere layers in the estimation of [CO_2] with 13 teeth.

The improvement of retrieval for higher optical power impels to search for better radiometric budget, either by improving detection or by increasing the power of the lasers. It is obvious that an operational mission should be photon limited in the future to reach the ultimate performance of DOFFS > 2 as pointed out by our study.

6.2 Spectral self-calibration

The Bayesian retrieval of [CO_2], from spectra affected by the above noise and a 0.001 cm^{-1} mismatch of the central wavelength of the comb, was simulated for combs of 3 and 13 teeth, at 6356 cm^{-1}, i.e. 1.57 µm. The error on the retrieved wavelength is given by Figure **26** to be 5.10^{-4} cm^{-1} with 3 teeth and 2.10^{-4} cm^{-1} with 13 teeth (this occurs when the comb is centered on the absorption line):

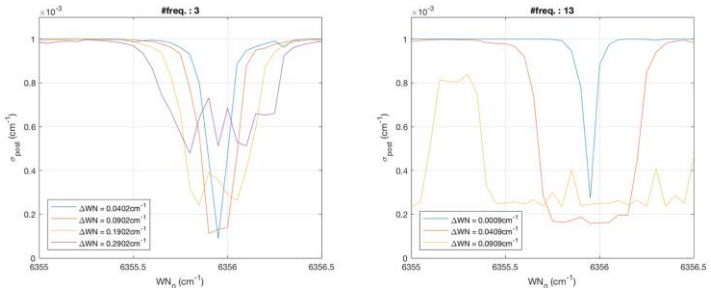

Figure 26. Comb central wavelength retrieval from SCALE spectra. Left: 3 tooth comb, right: 13 tooth com. ΔWN = frequency step, WN_0 = central frequency.

This is not as good as the A-SCOPE requirement (70 kHz) [9] but it allows to limit the [CO_2] error to 0.5% (2 ppm for 400ppm CO2 column mixing ratio), thanks to the spectral richness of the comb, as inferred from Figure **27**:

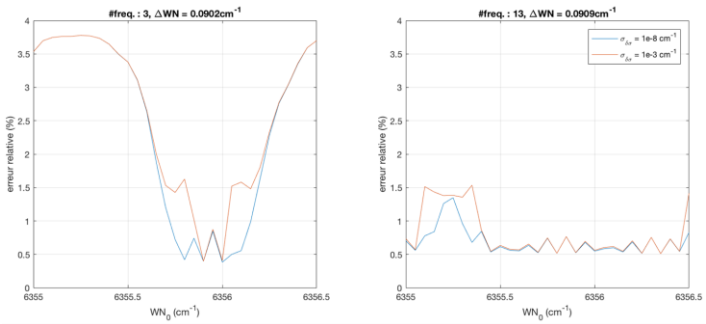

Figure 27. Impact of a wavelength calibration error of 10^{-3} cm^{-1} on [CO_2] error. Left: 3 tooth comb, right: 13 tooth com. ΔWN = frequency step, WN_0 = central frequency.

It is worth noting that the 2 ppm error include the effect of the radiometric noise. The weight of the spectral calibration is only 1.2 ppm in the total error budget. The spectral calibration retrieval can be thus considered as efficient.

7. CONCLUSIONS

CNES and ONERA propose a novel lidar concept, based on short frequency combs. Our recent works confirm the feasibility of single line spectroscopy and all its interest for molecule sounding in the atmosphere from space. The first advantage is to cancel the concern about spectral calibration of power laser emitters. The second one is to improve the information about the vertical profile. These aspects make short comb lidar a technical as well as a conceptual breakthrough that can be used for CO_2, but for other molecules as CH_4 or H_2O as well.

The device was mounted in the laboratory and the tests showed encouraging results.

Under CNES initiative the first space instrument of that kind (SCALE), fitted to a micro-satellite bus, takes a step beyond DIAL lidars, limited to DOFFS = 1 whatever their radiometric performance.

Our challenge in the next future will be to reach DOFFS > 2 by improving the detection process to the photon limit. Including the optimized configuration of the combs to better deal with unknowns like H_2O content, wavelength calibration, ground reflectivity and so forth, a CNES advance "phase 0" study will then complete this preliminary estimation of SCALE's retrieval capabilities.

ACKNOWLEDGEMENTS

The authors would like to thank ACRI ST for their works on the retrieval of [CO_2] from short comb spectra.

REFERENCES

[1] Ehret G., et al., "MERLIN; a French-German Space Lidar Mission Dedicated to Atmospheric Methane", Remote Sens. 2017, 9, 1052; doi:10.3390/rs9101052 (2017)
[2] Col., "Observing our future", 2018, http://www.tropomi.eu/, (17 July 2018)
[3] Pasternak F., Bernard P., Georges L., Pascal V., "The Microcarb instrument", Proc. SPIE 10562, International Conference on Space Optics — ICSO 2016, 105621P (25 September 2017)
[4] Cayla F.R., "L'interferomètre IASI", La météorologie 8ème série, 32, 23-39, 2001
[5] Smith W.L. Sr., Revercomb H.E., et al., « CrIS – Evolution of the Operational Advanced Sounder », 96th Annual AMS Meeting (10 -14 January 2016)

[6] Fischer H., et al., "MIPAS: an instrument for atmospheric and climate research", Atmos. Chem. Phys., 8, 2151–2188, 2008
[7] Abshire, J. B., Riris H., et al., "Pulsed airborne lidar measurements of atmospheric CO_2 column absorption", Tellus (2010), 62B, 770 - 783
[8] Ramanathan A., Mao J., Abshire J. B., Sun X., "CO_2 Sounder lidar : Retrieval Algorithm and Analysis Approach for airborne instrument and application to space instrument", IWGGMS-12, 9 June 2012, http://www.nies.go.jp/soc/events/iwggms12
[9] Col., "A-SCOPE Report for Assessment", ESA, SP-1313/1 (Nov. 2008)
[10] Singh U. N, et al., "Space-based active optical remote sensing of carbon dioxide column using high-energy two-micron pulsed IPDA lidar", ILRC28 (June 2017)
[11] Abshire J. B., et al., "Developing the CO2 Sounder lidar as a candidate for the ASCENDS Mission: an update", SPIE Remote Sensing, Paper 9645-4 (21 -24 September 2015)
[12] Coddington I, Swann W. C., Newbury N. R., "Coherent Multiheterodyne Spectroscopy Usign Stabilized Optical Frequency Combs", Physical Review Letters, PRL 100, 013902 (2008)
[13] Coddington I, Swann W. C., Newbury N. R., "Coherent dual-comb spectroscopy at high signal-to-noise ratio", Phys. Rev. A 82, 043817 – (12 October 2010)
[14] Mammez D., Cadiou E., Dherbecourt J-B., Raybaut M., Melkonian J-M., Godard A., Gorju G., Pelon J., Lefebvre M., "Multispecies transmitter for DIAL sensing of atmospheric water vapour, methane and carbon dioxide in the 2 µm region" Proc. SPIE 9645, Lidar Technologies, Techniques, and Measurements for Atmospheric Remote Sensing XI, 964507 (20 October 2015)
[15] Boudreau S., et al., "Chemical detection with hyperspectral lidar using dual frequency combs", Optics Express, 7411, Vol. 21. No. 6 (25 March 2013)
[16] Hébert P. J., Lemaître F., "Procédé de génération de peignes fréquentiels, module de génération associé, procédé de spectroscopie à distance et dispositif de spectroscopie associé", patent pending #17 54571, (23 May 2017)
[17] Hébert P. J., "Dispositif de spectroscopie à distance de type Lidar", patent #14 59660, (9 December 2016)
[18] Col., "Myriade-Evolution", https://myriade-evolutions.cnes.fr/ (20 February 2018)
[19] Nicholson J. W., et al., "High energy, 1572.3 nm pulses for CO2 LIDAR from a polarization-maintaining, very-largemode- area, Er-doped fiber amplifier", Optics Express Vol. 24, No. 17 (22 Aug 2016)
[20] Col., "SRM 2519a - High Resolution Wavelength Calibration Reference for 1530 nm -1565 nm Hydrogen Cyanide", Standard Reference Materials, SRM Online Request System, https://www-s.nist.gov/srmors/view_datafiles.cfm?srm=2519a, (2018)